Effect of parameter mismatch on the mechanism of chaos synchronization loss in coupled systems

V. Astakhov,[1] M. Hasler,[2] T. Kapitaniak,[3] A. Shabunin,[1] and V. Anishchenko[1]

[1]*Physics Department, Saratov State University, Astrachanskaya 83, 410071 Saratov, Russia*
[2]*Electrical Engineering Department, Swiss Federal Institute of Technology, CH-1015 Lausanne, Switzerland*
[3]*Division of Dynamics, Technical University of Lodz, Stefanowskiego 1/15, 90-924 Lodz, Poland*

Using the example of two coupled logistic maps, we investigate the effect of nonidentical subsystems on the bifurcations of saddle periodic orbits embedded in a symmetric chaotic attractor. These bifurcations determine the process of loss of chaos synchronization. We show that if bifurcations conditioned by the symmetry of the system take part in the synchronization loss process, nonidentity changes the bifurcation scenario of the transition to a nonsynchronous regime. In this case, for example, the transition to the bubbling behavior is determined not by bifurcation of an orbit embedded in the chaotic attractor but by the smooth shift of it and the saddle-repeller bifurcation of the birth of new orbits in the vicinity of the quasisymmetric region. [S1063-651X(98)10909-1]

PACS number(s): 05.45.+b

I. INTRODUCTION

Interacting identical systems may have completely identical chaotic motions [1–9]. This regime of cooperative behavior is one kind of chaos synchronization [10–14]. The complete synchronization regime corresponds to a chaotic attractor that is located in the symmetric subspace $x_1 = x_2$ of the whole phase space of the coupled systems. When the system exits the synchronous region, the chaotic attractor loses its stability in the direction that is normal to the symmetric subspace. This occurs according to a determined scenario [15,16]. As a rule, the bubbling and the riddling transitions accompany the loss of stability of the symmetric chaotic attractor [15–23].

The loss of chaos synchronization is directly connected with bifurcations of saddle periodic orbits embedded in the chaotic attractor [18,24–27]. In [26], e.g., it was demonstrated that the loss of phase synchronization begins with a saddle-node bifurcation of an unstable periodic trajectory embedded in the chaotic attractor. As a result, a specific intermittency regime (eyelet intermittency [26]) appears. In [24] it was found that a subcritical pitchfork bifurcation of the saddle point embedded in the symmetric chaotic attractor induces the riddling transition.

In [27] we investigated the bifurcation mechanism of the loss of stability of synchronous chaotic motions in coupled logistic maps:

$$x_{n+1} = \lambda_1 - x_n^2 + \epsilon_1(x_n^2 - y_n^2), \quad y_{n+1} = \lambda_2 - y_n^2 + \epsilon_2(y_n^2 - x_n^2) \tag{1}$$

(where x_n, y_n are dynamic variables, $\lambda_{1,2}$ are controlling parameters of the partial systems, and $\epsilon_{1,2}$ are coupling coefficients). The following properties were proved for the symmetric case ($\lambda_1 = \lambda_2 = \lambda$ and $\epsilon_1 = \epsilon_2 = \epsilon$).

In the system (1) the synchronization region has a finite interval. The stability loss of the symmetric one-bound chaotic attractor A^0 in the normal direction occurs for both decreasing and increasing coupling coefficient ϵ. The synchronization loss is induced by bifurcations of saddle orbits $2^N C^0$ ($2N$ is the period of the orbit, $N = 0,1,2, \dots$) that are embedded in the chaotic attractor and form its skeleton. In the cases of coupling both increasing and decreasing the loss of stability begins with a bifurcation of the saddle point C^0, which induces the bubbling transition in the system.

At ϵ decreasing the saddle point C^0 undergoes period-doubling bifurcation. As a result it becomes a repeller and the saddle period-2 orbit $2C^1$ appears in its vicinity outside the symmetric subspace. This bifurcation induces the bubbling transition in the system. For ϵ decreasing further the saddle orbits $2^N C^0$ of higher periods undergo the same bifurcations. This enforces the bubbling phenomenon.

Then the saddle orbit $2C^1$ located outside the symmetric subspace undergoes a bifurcation. It becomes stable and a pair of period-2 saddle orbits symmetric to each other appears in its vicinity (for an inverse parameter change this bifurcation is the subcritical pitchfork bifurcation). The bifurcation of the orbit $2C^1$ induces the riddling transition in the system. For a further decrease of the coupling the chaotic attractor gradually ''loses'' its basins and transforms into a chaotic saddle.

In the case of the coupling increasing the point C^0 undergoes a pitchfork bifurcation. As a result it becomes a repeller and in its vicinity a pair of saddle points C_1^0 and C_2^0 symmetric to each other appear. This bifurcation induces the bubbling transition. For a further increase of ϵ other saddle orbits $2^N C^0$ undergo period-doubling bifurcations similarly to the case of coupling decreasing. The riddling phenomenon of the A^0 basins is a result of the bifurcation of the saddle points C_1^0 and C_2^0. They become stable and in their vicinities saddle orbits of double period appear (for an inverse parameter change this bifurcation is the subcritical period-doubling bifurcation).

In the case of the coupling both decreasing and increasing the bifurcation scenarios of the synchronization loss are very similar. The only difference is that at weak coupling C^0 undergoes a period-doubling bifurcation, but at strong coupling

a pitchfork bifurcation. Other saddle orbits $2^N C^0$ undergo period-doubling bifurcations in both cases. For decreasing ϵ the process of riddling basins of A^0 begins with the pitchfork bifurcation of the orbit $2C^1$, but for increasing ϵ with the period-doubling bifurcations of C_1^0 and C_2^0.

For the investigation of the complete synchronization phenomenon identical interacting systems are usually used as mathematical models. Then, obtained in the framework of such an idealization, the results are applied to explain the behavior of real experimental systems. If the regime of synchronization is stable and rough for the mathematical model it is observable in experiment. Intervals of synchronization on the coupling parameter are practically similar for identical and slightly mismatched systems. In this sense the behaviors of the identical and slightly mismatched systems correspond to each other. However, when we investigate more exact effects such as the mechanism of synchronization loss from the point of view of bifurcations of saddle periodic orbits embedded in the chaotic attractor, differences in the scenario for identical and slightly nonidentical systems can be observed in some cases. This situation can take place when the symmetry-breaking bifurcations take part in the process of synchronization loss. For example, this is the pitchfork bifurcation. From the bifurcation and catastrophe theory it is well known (see [28–30]) that the point of this bifurcation is the cusp catastrophe. For a slight nonidentity between interacting systems the bifurcation is eliminated in certain ways. Nonidentity can qualitatively change the behavior of orbits depending on the parameters of the system.

According to the discussion above, we suppose that it is very important to investigate the influence of the nonidentity of coupled systems on the bifurcation scenario of the chaotic synchronization loss. Some aspects connected with the asymmetry influence were discussed in [18,24,23].

In this work we study the parameter mismatch effect on the bifurcation scenario of the synchronization loss of the system (1) with $\epsilon_1 = \epsilon_2 = \epsilon$ and the detuning of the parameters $\lambda_{1,2}$: $\lambda_1 = \delta\lambda$ and $\lambda_2 = \lambda$ (where δ is the detuning parameter). We consider the synchronization loss for both decreasing and increasing coupling coefficient ϵ. For a small value of δ we investigate bifurcations of unstable periodic orbits, which lead to breaking of the regime of nearly identical chaotic oscillations of coupled systems. We demonstrate that for a slight nonidentity the elimination of bifurcations conditioned by the symmetry of the system leads to a change of the scenario of the transition from the regime of nearly identical chaotic oscillations to bubbling behavior.

For decreasing ϵ a period-doubling bifurcation of the saddle point C^0 induces the transition to the bubbling behavior. After this bifurcation a rebuilding of the phase space structure in the vicinity of A^0 occurs. Namely, in the quasisymmetric region the repeller C^0 appears and outside this region a saddle orbit $2C^1$ appears. Stable manifolds of the saddle $2C^1$ lean on the repeller C^0 and unstable manifolds leave to the quasisymmetric region. The appearance of such a structure changes the character of motions from nearly identical oscillations to the bubbling behavior.

For an increase of the coupling the scenario of the transition to the bubbling behavior is different. With increasing ϵ first there is a gradual displacement of the saddle C^0 in the normal direction. It leaves the quasisymmetric region. Other

saddle orbits $2^N C^0$ practically do not change their locations. Then a saddle-repeller bifurcation takes place in the system. In the vicinity of the quasisymmetric region a repeller C_r^0 and a saddle C_s^0 appear. For a further increase of ϵ the fixed points diverge. The repeller C_r^0 enters the quasisymmetric region and the saddle C_s^0 moves away from it. As a result the structure of the phase space in the vicinity of A^0 is the same as in the case of decreasing coupling. In the quasisymmetric region there is the repeller C_r^0 on which stable manifolds of the saddles C^0 and C_s^0 lean. Their unstable manifolds leave the quasisymmetric region. This phase space structure also leads to the bubbling behavior. In the case of identical systems this structure appears as a result of the pitchfork bifurcation of the saddle point C^0.

In Sec. II we describe invariant and attracting sets of the system (1). In Sec. III we demonstrate several regimes in the vicinity of the synchronization region. An analysis of the bifurcation of unstable periodic orbits that induce the loss of synchronization is considered in Sec. IV. In Sec. V we compare the results obtained with the symmetric case.

II. INVARIANT AND ATTRACTING SETS

We suppose that $0 < \lambda \leq 2$ and $0 < \delta \leq 1$. Under these conditions, it is easy to see that the square $\{(x,y) \mid |x| \leq \lambda, |y| \leq \lambda\}$ is invariant under the transformation (1). In the following we shall restrict our dynamical system (1) to this square.

Lemma 1. For the square $\{(x,y) \mid |x| \leq \lambda, |y| \leq \lambda\}$ the inequality $|x+y| \leq 2\lambda - |x-y|$ holds.

Proof. If $x \geq y$,

$$|x+y| = |2x - (x-y)| \leq 2|x| - |x-y| \leq 2\lambda - |x-y|.$$

If $y > x$,

$$|x+y| = |2y - (y-x)| \leq 2|y| - |y-x| \leq 2\lambda - |x-y|.$$

Theorem 1. If $\epsilon \in (\frac{1}{2} - 1/4\lambda, \frac{1}{2} + 1/4\lambda)$, the stripe

$$\left\{ (x,y) \left| |x-y| \leq \frac{1 - 2\lambda|1 - 2\epsilon|}{2|1 - 2\epsilon|} \right. \right.$$

$$\left. \times \left(-1 + \sqrt{1 + \frac{4\lambda|\delta - 1||1 - 2\epsilon|}{(1 - 2\lambda|1 - 2\epsilon|)^2}} \right) \right\}$$
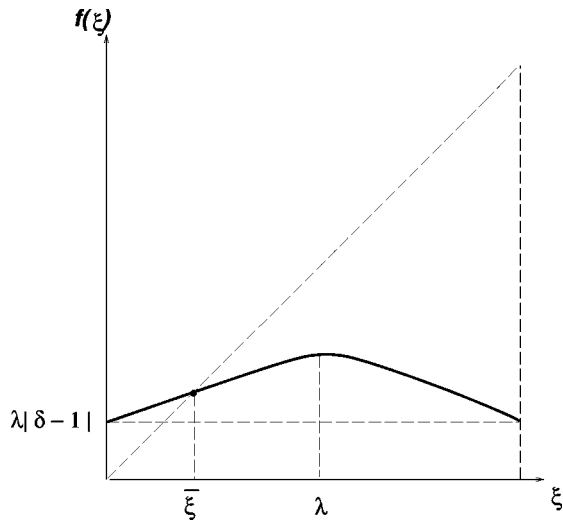
(2)

is an attracting set. If δ is close to 1, this is approximately the stripe

$$\left\{ (x,y) \left| |x-y| \leq \frac{\lambda|\delta - 1|}{1 - 2\lambda|1 - 2\epsilon|} \right. \right\}.$$

(3)

Proof. Subtracting the two equations of the system (1) leads to

$$|x_{n+1} - y_{n+1}| \leq |\lambda_1 - \lambda_2| + |1 - 2\epsilon||x_n^2 - y_n^2|$$

$$= \lambda|\delta - 1| + |1 - 2\epsilon||x_n + y_n||x_n - y_n|.$$

Due to the lemma

FIG. 1. Plot of the function $f(\xi)$.

$$|x_{n+1} - y_{n+1}| \leq \lambda |\delta - 1| + |1 - 2\epsilon| |2\lambda - |x_n - y_n|| |x_n - y_n|. \tag{4}$$

Thus

$$|x_{n+1} - y_{n+1}| \leq f(|x_n - y_n|), \tag{5}$$

where $f(\xi) = \lambda |\delta - 1| + |1 - 2\epsilon| (2\lambda - \xi) \xi$ for $0 \leq \xi \leq 2\lambda$.

The function is represented in Fig. 1 for the case $|1 - 2\epsilon| 2\lambda \leq 1$. It is bounded by the increasing function

$$g(\xi) = \begin{cases} f(\xi), & \xi \leq \lambda \\ f(\lambda), & \xi > \lambda, \end{cases}$$

which has the same fixed point as f in $0 \leq \xi \leq \lambda$,

$$\bar{\xi} = \frac{1 - 2\lambda |1 - 2\epsilon|}{2|1 - 2\epsilon|} \left(-1 + \sqrt{1 + \frac{4\lambda |\delta - 1| |1 - 2\epsilon|}{(1 - 2\lambda |1 - 2\epsilon|)^2}} \right). \tag{6}$$

From $|x_{n+1} - y_{n+1}| \leq g(|x_n - y_n|)$ and the monotonicity of g we get

$$|x_n - y_n| \leq g^{(n)}(|x_0 - y_0|). \tag{7}$$

However, the iterates of g converge to $\bar{\xi}$ and thus

$$\limsup_{n \to \infty} |x_n - y_n| \leq \bar{\xi}, \tag{8}$$

which proves that the stripe $|x - y| \leq \bar{\xi}$ is an attracting set.

The detuning between parameters ($\delta \neq 1$) destroys the symmetry of the system (1). However, Theorem 1 shows that in slightly nonidentical subsystems and suitable coupling constants, the two systems approximately synchronize.
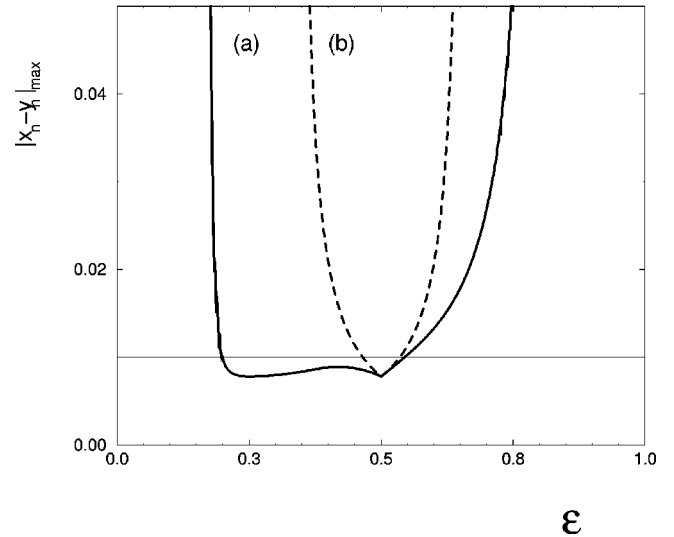

FIG. 2. Plot of the maximum values $|x_n - y_n|$ for $n = 10\,000$ as a function of the coupling parameter ϵ at $\lambda = 1.56$ and $\delta = 0.995$ (a). The straight line indicates the threshold value $\Delta = 0.01$. The dashed line (b) gives the theoretical asymptotic bound on $|x_n - y_n|$ obtained using theorem 1.

III. DYNAMICS IN THE VICINITY OF THE SYNCHRONIZATION REGION

In this section we present an ''experimental'' description of oscillating regimes in the asymmetric system (1) depending on the coupling coefficient ϵ at $\lambda = 1.56$. This value of λ corresponds to the one-bound chaotic attractor in the individual system. In the framework of the present description we shall call the chaotic regime synchronous if $|x_n - y_n| < \Delta$ at any moment of time n, where Δ is a suitable given value that is small with respect to the intensity of the chaotic oscillation. In the following we shall take $\delta \geq 0.995$ and $\Delta = 0.01$. This condition allows us to evaluate the interval of values of the parameter ϵ, where for the fixed value of the detuning δ the systems demonstrate nearly identical chaotic oscillations. Figure 2 shows the plot of maximal values $|x_n - y_n|$ for $n = 10\,000$ as a function of ϵ [curve (a)]. The straight line indicates the threshold value Δ. The dashed line [curve (b)] gives the theoretical asymptotic bound on $|x_n - y_n|$ obtained using Theorem 1. It is quite good in the middle of the synchronizing interval, but it fails at the extremities of this interval.

From Fig. 2 we can see that the coupled systems have almost identical trajectories in the interval of ϵ values from approximately 0.2 to 0.55. The difference between the state variables does not exceed the given threshold $\Delta = 0.01$. When ϵ leaves this interval of values, $|x_n - y_n|$ increases rapidly. Figures 3 and 4 represent time series $(x_n - y_n)$ when ϵ decreases and increases, respectively.

Decreasing the coupling constant, we observe a smooth transition from the synchronous chaotic oscillation [Fig. 3(a)] to the bubbling behavior [Fig. 3(b)]. With a further decrease of the coupling the bubbling behavior becomes more developed. Then a period-2 out-of-phase oscillation regime appears [Fig. 3(c)]. The time of the transient process to the stable period-2 orbit has a sensitive dependence on the initial condition and it can reach several 10^6 iterations.
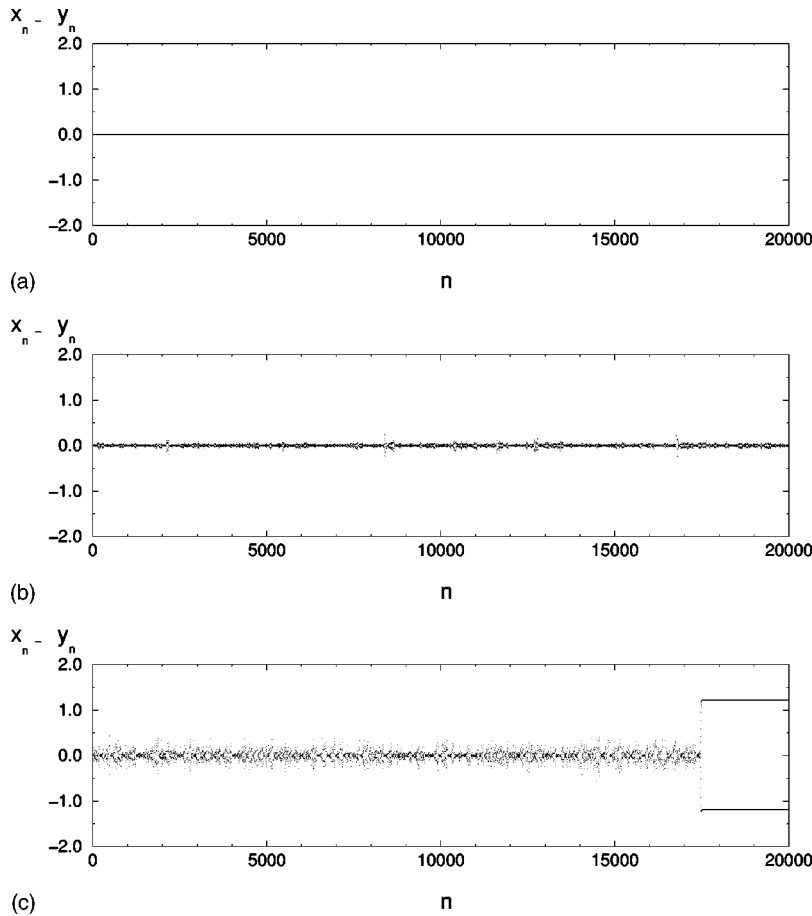
Increasing the coupling, we observe an almost identical

FIG. 3. Time series $(x_n - y_n)$ of the system (1) at $\delta = 0.995$ and $\lambda = 1.56$ for (a) $\epsilon = 0.22$, (b) $\epsilon = 0.157$, and (c) $\epsilon = 0.143$.

process of loss of chaos synchronization if it is estimated by phase portraits and time series $(x_n - y_n)$ (Fig. 4). The bubbling behavior is also observed in the system, which is intensified with increasing ϵ. After this the transition to stable fixed point outside the quasisymmetric region takes place [Fig. 4(c)]. The time of the transition process to the stable fixed point has the same sensitive dependence on the initial conditions as in the case of weak coupling.

Comparing the behaviors of the system (1) at $\delta = 0.995$ and $\delta = 1$ [27], we see a good qualitative correspondence. The regime of complete synchronization correspond to nearly identical chaotic oscillations. The bubbling transitions in the symmetric system correspond to the appearance of the bubbling behavior in the system with mismatch. Furthermore, the parameter of coupling changing the same stable orbits appears in both the symmetric and asymmetric systems. In the asymmetric systems there are no riddled basins, but one can observe the sensitive dependence of the transition process time on initial conditions.

However, comparing the results quantitatively, one needs to take into account the following. For decreasing coupling the value $|x_n - y_n|$ exceeds the chosen threshold value Δ nearly at the same value of ϵ that corresponds to the bubbling transition in the identical systems. For increasing coupling the corresponding values of ϵ are very different. Below we will show that this difference of changing of left and right boundaries of the synchronization interval is a result of the difference of behavior of unstable periodic orbits embedded in the chaotic attractor, which takes place for decreasing and increasing ϵ. This difference appears as a result of the elimi-

nation of the bifurcation conditioned by the symmetry of the system. Let us consider the behavior of some saddle periodic orbits embedded in the chaotic attractor A^0 when chaos synchronization is lost.

IV. BEHAVIOR OF UNSTABLE PERIODIC ORBITS FOR A LOSS OF CHAOS SYNCHRONIZATION

As it was mentioned above, at $\delta = 1$ and $\lambda = 1.56$ the one-bound chaotic attractor A^0 located in the symmetric subspace $x_n = y_n$ corresponds to the regime of chaos synchronization. For coupling both increasing and decreasing the saddle orbits $2^N C^0$ embedded in A^0 undergo bifurcations that lead to a loss of chaotic synchronization. In the cases of coupling increasing and decreasing the bubbling transition is determined by different bifurcations of the saddle point C^0. For decreasing ϵ it undergoes a period-doubling bifurcation, but for increasing ϵ the pitchfork bifurcation. Let us consider the influence of the nonidentity on the bifurcation scenario for coupling both increasing and decreasing.

A small parameter mismatch ($\delta \neq 1$) breaks the symmetry of the system but does not lead to qualitative changes of the structure of the chaotic attractor A^0. In the above-mentioned interval of ϵ (0.2–0.55) the chaotic attractor A^0 is slightly deformed. The bound in which the phase point evolves is located near the symmetric subspace (we call this region the quasisymmetric region). In the interval of parameter values considered the orbits embedded in the chaotic attractor are saddles.

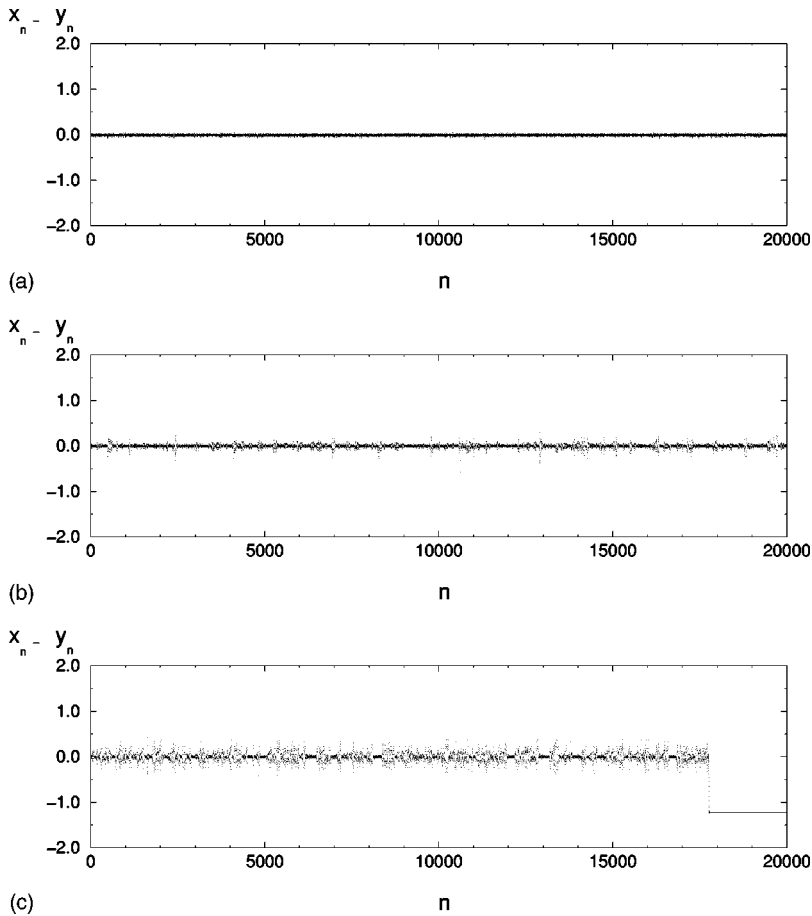Figure 5(a) shows saddle orbits C^0, $2C^0$, and $4C^0$ at the

FIG. 4. Time series $(x_n - y_n)$ of the system (1) at $\delta = 0.995$ and $\lambda = 1.56$ for (a) $\epsilon = 0.803$, (b) $\epsilon = 0.843$, and (c) $\epsilon = 0.857$.

value $\epsilon = 0.22$, which is within the region of chaos synchronization. We can see that they lie almost in the subspace $x_1 = x_2$.

Decreasing the coupling coefficient, the unstable periodic orbits do not leave the quasisymmetric region; their coordinates are practically unchanged. At $\epsilon = 0.2038$, 0.1648, 0.1599, 0.1615, and 0.1597 orbits C^0, $2C^0$, $4C^0$, $8C^0$, and $16C^0$, respectively, undergo period-doubling bifurcations. These bifurcations lead to a loss of chaos synchronization, which begins with the bifurcation of the saddle C^0. At $\epsilon = 0.2038$ the saddle's second eigenvalue is equal to -1. As a result C^0 transforms to a repeller. In the neighborhood of C^0 a saddle periodic orbit $2C^1$ gradually appears. With the decrease of coupling the orbit points smoothly go away from the quasisymmetric region. Now, in the quasisymmetric region, besides saddles there is a repeller. Outside this region there is a saddle $2C^1$. In Fig. 5(b) stable (W^s) and unstable (W^u) manifolds of the saddle $2C^1$ are built. As it is seen from the figure, when the phase point enters a small neighborhood of C^0 it is repelled from the quasisymmetric region along the stable manifold W^s. If the phase point reaches the vicinity of the saddle $2C^1$ it returns along the unstable manifolds W^u to the quasisymmetric region. The appearance of such a structure of the repeller, the saddle, and its stable and unstable manifolds in the vicinity of A^0 changes the character of motions from nearly identical oscillations of systems to the bubbling behavior. After the bifurcation of the saddle C^0 the regime of bubbling behavior appears in the system.

Then, at the above-mentioned values of ϵ saddle orbits with higher periods ($2C^0$, $4C^0$, $8C^0$, and $16C^0$) embedded

in the chaotic set A^0 undergo period-doubling bifurcations. They transform to repellers and saddle orbits of double periods gradually appear in their respective neighborhoods [Fig. 5(c)]. These bifurcations intensify the bubbling phenomenon.

At $\epsilon = 0.1483$ a saddle-node bifurcation takes place. In the neighborhood of the saddle periodic orbit $2C^1$ the stable periodic orbit $2C_N^1$ and the saddle periodic orbit $2C_s^1$ appear [Fig. 5(d)]. This bifurcation completes the process of the loss of chaos synchronization. From any initial conditions near the chaotic set A^0 the trajectory converges to $2C_N^1$. However, the time of the transient process depends on the initial condition very sensitively and in a complicated way. The transient process has the form of an on-off intermittency.

Now let us consider the saddle periodic orbits embedded in A^0 when the coupling coefficient increases. When ϵ exceeds the value 0.55 the saddle point C^0 exits the quasisymmetric region. The other saddle periodic orbits stay there. Their coordinates remain practically unchanged. Figure 6(a) shows the positions of the saddle periodic orbits. Consequently, the attractor skeleton is deformed and protrudes from the quasisymmetric region. This leads to an increase of the difference between the values of the dynamical variables $|x_n - y_n|$ for increasing ϵ before the bifurcations of the saddles. At $\epsilon = 0.8069$ the saddle-repeller bifurcation (eigenvalue $+1$) takes place. The repeller C_r^0 and the saddle C_s^0 appear in the vicinity of the quasisymmetric region. As the coupling ϵ increases, these fixed points diverge. The repeller C_r^0 enters the quasisymmetric region and the saddle point C_s^0 moves away from it. From Fig. 6(b) one can see that as a
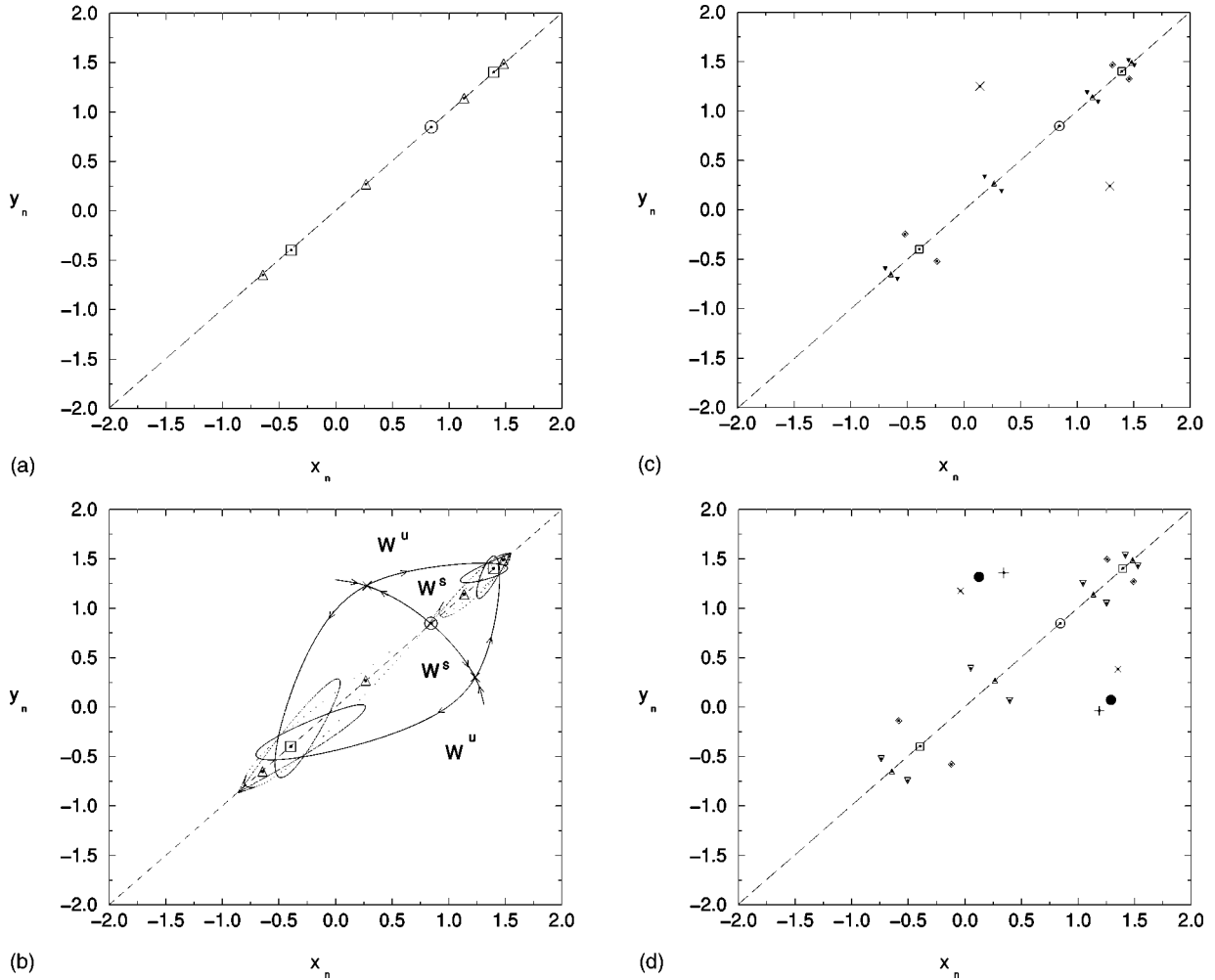
FIG. 5. Periodic orbits [C^0 ($\bigcirc$), $2C^0$ ($\square$), $4C^0$ ($\triangle$), $4C^2$ ($\diamond$), $8C^4$ ($\triangledown$), $2C^1$ ($\times$), $2C_s^1$ (+), $2C_N^1$ ($\bullet$)] at $\lambda=1.56$ and $\delta=0.995$ for (a) $\epsilon=0.22$, (b) $\epsilon=0.17$ (W^s, W^u are stable and unstable manifolds of the saddle orbit $2C^1$), (c) $\epsilon=0.157$, and (d) $\epsilon=0.143$. Dots inside symbols indicate the precise location of the orbits. The dashed line is the symmetric subspace $x_n = y_n$.

result, in the vicinity of A^0 the structure of the phase space is the same as in the case of decreasing ϵ [see Fig. 5(b)]. The quasisymmetric region contains the repeller C_r^0, on which stable manifolds W_1^s and W_2^s of the saddles C^0 and C_s^0 lean. Their unstable manifolds (W_1^u and W_2^u) lead to the quasisymmetric region. Formation of this structure leads to the bubbling behavior. With the change of the coupling at $\epsilon = 0.8353, 0.8401, 0.8386,$ and 0.8404 the saddle periodic orbits $2C^0$, $4C^0$, $8C^0$, and $16C^0$, respectively, undergo a period-doubling bifurcation. They transform to repellers and periodic orbits of double period appear in their neighborhood [Fig. 6(c)]. These bifurcations lead to a more developed bubbling behavior. At $\epsilon=0.8448$ the maximal eigenvalue of the saddle fixed point C^0 becomes equal to -1. As a result C^0 transforms to a stable fixed point and in its neighborhood the saddle orbit of doubled period $2C_1^s$ gradually appears. For a reverse parameter change this bifurcation corresponds to the subcritical period-doubling bifurcation. At $\epsilon=0.8494$ the fixed point C_s^0 undergoes a similar bifurcation. As a result it becomes a stable fixed point and in its vicinity the saddle periodic orbit $2C_2^s$ gradually appears [Fig. 6(d)]. This bifurcation of the saddle fixed point C^0 completes the process of the loss of chaos synchronization. From any initial condi-

tions near the chaotic set A^0 the trajectory converges to the stable fixed point C^0. The time of the transient process depends on the initial condition very sensitively and in a complicated way.

V. COMPARISON WITH THE SYMMETRIC CASE

Let us consider the bifurcation diagrams on the base of the saddle point C^0 presented in Fig. 7. They show in detail the similarities and differences of the main stages of the chaos synchronization loss process in the symmetric and nonsymmetric cases.

In the symmetric situation [$\delta=1$, Fig. 7(a)], for decreasing coupling the saddle point undergoes a period-doubling bifurcation at $\epsilon=0.2043$. As a result C^0 becomes a repeller and in its vicinity the saddle orbit $2C^1$ appears. It is symmetric with respect to the coordinate transformation $(x_n, y_n) \leftrightarrow (y_n, x_n)$. At $\epsilon=0.1533$ the maximal eigenvalue of the saddle orbit $2C^1$ enters the unit circle through $+1$. It becomes stable and a pair of saddle symmetric orbits $2C_s^1$ and $2C_s^2$ gradually appear. The bifurcation of the saddle point C^0 induces the bubbling transition and the bifurcation of the saddle orbit $2C^1$ induces the riddling transition [27].
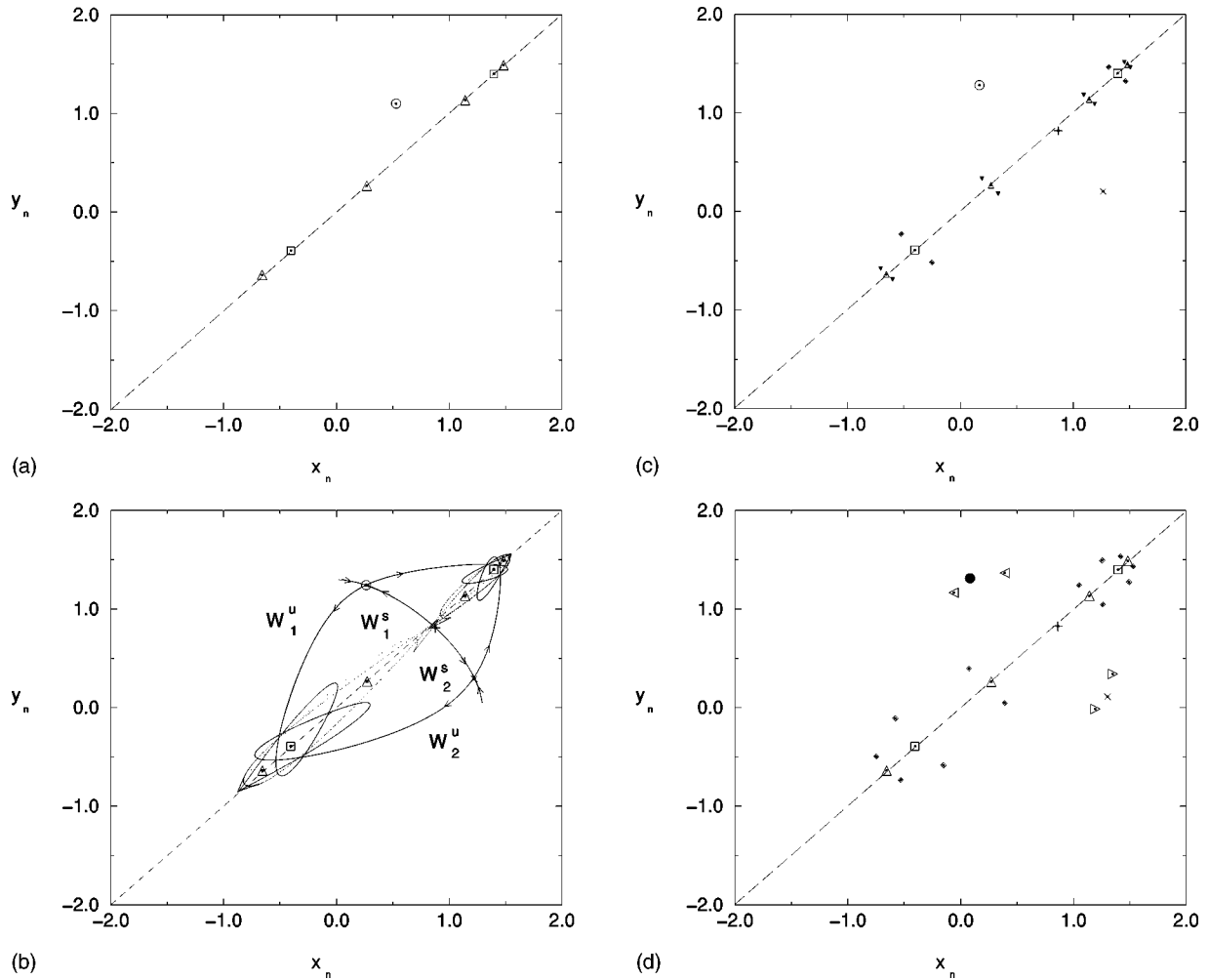
FIG. 6. Periodic orbits [C^0 ($\bigcirc$), $2C^0$ ($\square$), $4C^0$ ($\triangle$), $4C^2$ ($\diamond$), $8C^4$ (∇), C_s ($\times$), C_r ($+$), $2C_1^s$ ($\triangleleft$), $2C_2^s$ ($\triangleright$), C^0 node ($\bullet$)] at $\lambda=1.56$ and $\delta=0.995$ for (a) $\epsilon=0.803$, (b) $\epsilon=0.83$ ($W_1^s, W_1^u, W_2^s, W_2^u$ are stable and unstable manifolds of the saddles C^0 and C_s^0, respectively), (c) $\epsilon=0.843$, and (d) $\epsilon=0.857$. Dots inside symbols indicate the precise location of the orbits. The dashed line is the symmetric subspace $x_n = y_n$.

In the asymmetric case [$\delta=0.995$, Fig. 7(b)], for decreasing coupling the saddle point C^0 undergoes also a period-doubling bifurcation at almost the same value $\epsilon=0.2038$. However, the saddle orbit $2C^1$ does not undergo any bifurcation with a further decrease of the coupling. For weak asymmetry the loss of the chaos synchronization is terminated at almost the same value of the coupling coefficient ($\epsilon=0.1483$) at which the riddling transition in the symmetric system takes place, but as a result of another bifurcation, the saddle-node bifurcation. The stable periodic orbit $2C_N^1$ and the saddle orbit $2C_s^1$ appear in the vicinity of the saddle orbit $2C^1$. After this bifurcation the trajectory converges to $2C_N^1$ from any initial conditions near the chaotic set A^0.

In the symmetric system [Fig. 7(a)], for increasing coupling the saddle point C^0 undergoes a symmetry-breaking bifurcation. At $\epsilon=0.7957$ its minimal eigenvalue becomes $+1$. As a result the point C^0 transforms to a repeller in the vicinity of which outside the symmetric subspace saddle fixed points C_1^1 and C_2^1 gradually appear. This bifurcation induces the bubbling transition in the system. At $\epsilon=0.8467$ the maximal eigenvalue of the saddle points C_1^1 and C_2^1 enters the unit circle through -1. They become stable fixed

points and in their vicinity saddle orbits of double period appear. This bifurcation of the saddle points C_1^1 and C_2^1 induces the riddling transition in the system.

In the asymmetric system [Fig. 7(b)], for increasing coupling the saddle point C^0 smoothly exits the quasisymmetric region. At $\epsilon=0.8069$ (at about this value the symmetry-breaking bifurcation takes place in the symmetric system) the saddle-repeller bifurcation (eigenvalue $+1$) takes place. The repeller C_r^0 and the saddle point C_s^0 appear in the vicinity of the quasisymmetric region. With a further increase of coupling the repeller enters the quasisymmetric region and the saddle point moves away from it. Then the bubbling behavior appears. At $\epsilon=0.8448$ and 0.8494 the maximal eigenvalue of the saddle fixed points C^0 and C_s^0, respectively, is equal to -1. C^0 and C_s^0 become stable fixed points. In their vicinity the saddle orbits of the double period $2C_1^s$ and $2C_2^s$ gradually appear. The bifurcation of the saddle C^0 completes the process of chaos synchronization loss.

Thus, if the bubbling transition in the symmetric system is induced by "uneliminated" bifurcation (the period-doubling bifurcation of the saddle C^0 for a coupling decrease) weak asymmetry does not influence the bifurcation scenario of the
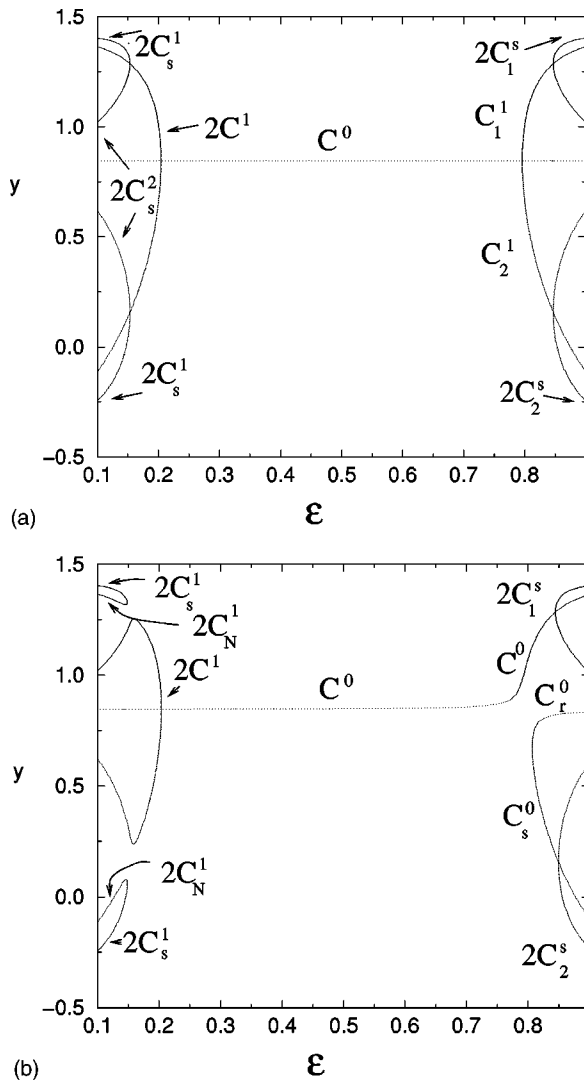
FIG. 7. Bifurcation diagrams of system (1) at $\lambda = 1.56$ for (a) the symmetry case $\delta = 1.0$ and (b) the nonsymmetric case $\delta = 0.995$.

bifurcation of the saddle C^0, but after the saddle-repeller bifurcation of the birth of new unstable points, namely, the repeller C_r^0 and the saddle C_s^0. The completion of the process of chaos synchronization loss occurs according to a different scenario in the symmetric and nonsymmetric systems. For decreasing coupling a slight nonidentity eliminates the bifurcation of the saddle $2C^1$. In addition, the saddle-node bifurcation of the new stable period-2 orbit $2C_N^1$ takes place. Starting from the vicinity of A^0, phase trajectories move to this stable orbit. For increasing coupling the loss of synchronization in the nonsymmetric system is completed by the bifurcation of the saddle C^0. After the bifurcation the point C^0 becomes stable.

VI. CONCLUSIONS

In this work, using the example of two coupled logistic maps, we investigate the influence of nonidentity on the mechanism of the chaos synchronization loss from the point of view of bifurcations of saddle orbits embedded in a chaotic attractor. We demonstrate that if bifurcations conditioned by the symmetry of the system take part in the synchronization loss process, nonidentity changes the bifurcation scenario of the transition to a nonsynchronous regime. In this case the transition to the bubbling behavior is determined not by the bifurcation of an orbit embedded in the chaotic attractor but by the saddle-repeller bifurcation of the new orbits in the vicinity of the quasisymmetric region. The completion of the chaos synchronization loss can be conditioned also by the saddle-node bifurcation of appearance of a new stable orbit. We must note that on all stages of chaos synchronization loss a slight asymmetry of the system does not change qualitatively the structure of the phase space, but the scenario of its formation becomes another one if at $\delta = 1$ bifurcations conditioned by the symmetry of the system take place.

transition to the bubbling behavior. If the bubbling transition is determined by the bifurcation conditioned by the symmetry of the system (the pitchfork bifurcation of the saddle C^0 for the coupling increase) the weak nonidentity of the subsystems eliminates it and the bubbling behavior appears according to another scenario. The determined structure of the phase space in the vicinity of A^0 forms not as a result of the

[1] T. Yamada and H. Fujisaka, Prog. Theor. Phys. **70**, 1240 (1983).
[2] A. S. Pikovsky, Z. Phys. B **55**, 149 (1984).
[3] S. P. Kuznetsov, Izv. Vyssh. Uchebn. Zaved. Radiofiz. **28**, 991 (1985).
[4] V. S. Afraimovich, N. N. Verichev, and M. I. Rabinovich, Radiophys. Quantum Electron. **29**, 795 (1986).
[5] V. V. Astakhov, B. P. Bezruchko, V. I. Ponomarenko, and E. P. Seleznev, Izv. Vyssh. Uchebn. Zaved. Radiofiz. **31**, 627 (1988).
[6] L. M. Pecora and T. L. Carroll, Phys. Rev. Lett. **64**, 821 (1990).
[7] T. Endo and L. O. Chua, Int. J. Bifurcation Chaos Appl. Sci. Eng. **1**, 701 (1991).
[8] M. de Sousa Viera, A. J. Lichtenberg, and M. A. Lieberman, Phys. Rev. A **46**, 7359 (1992).
[9] T. Kapitaniak, Phys. Rev. E **50**, 1642 (1994).
[10] V. S. Anishchenko, T. E. Vadivasova, D. E. Postnov, and M. A. Safonova, Radio Eng. Electron. **36**, 338 (1991).
[11] P. S. Landa and M. G. Rosenblum, Sov. Phys. Dokl. **37**, 237 (1992).
[12] L. Kocarev, A. Shang, and L. O. Chua, Int. J. Bifurcation Chaos Appl. Sci. Eng. **3**, 479 (1993).
[13] M. Rosenblum, A. Pikovsky, and J. Kurths, Phys. Rev. Lett. **76**, 1804 (1996).

[14] N. F. Rulkov, K. M. Sushchik, L. S. Tsimring, and H. D. I. Abarbanel, Phys. Rev. E **51**, 980 (1995).

[15] P. Ashwin, J. Buescu, and I. Stewart, Phys. Lett. A **193**, 126 (1994).

[16] S. C. Venkataramani, B. R. Hunt, and E. Ott, Phys. Rev. E **54**, 1346 (1996).

[17] H. Fujisaka and T. Yamada, Prog. Theor. Phys. **74**, 917 (1985).

[18] A. S. Pikovsky and P. Grassberger, J. Phys. A **24**, 4587 (1991).

[19] Y. Maistrenko and T. Kapitaniak, Phys. Rev. E **54**, 1 (1996).

[20] E. Ott and J. C. Sommerer, Phys. Lett. A **193**, 126 (1994).

[21] E. Ott, J. C. Sommerer, J. C. Alexander, I. Kan, and J. A. Yorke, Physica D **76**, 384 (1994).

[22] N. Platt, E. A. Spigel, and C. Tresser, Phys. Rev. Lett. **70**, 279 (1993).

[23] M. Hasler and Y. Maistrenko, IEEE Trans. Circuits Syst., I: Fundam. Theory Appl. **44**, 856 (1997).

[24] Y.-C. Lai, C. Grebogi, J. A. Yorke, and S. C. Venkataramani, Phys. Rev. Lett. **77**, 55 (1996).

[25] N. F. Rulkov and M. M. Suschik, Phys. Lett. A **214**, 145 (1996).

[26] A. Pikovsky, G. Osipov, M. Rosenblum, M. Zaks, and J. Kurths, Phys. Rev. Lett. **79**, 47 (1997).

[27] V. Astakhov, A. Shabunin, T. Kapitaniak, and V. Anishchenko, Phys. Rev. Lett. **79**, 1014 (1997).

[28] V. I. Arnold, *Theory of Ordinary Differential Equations* (Nauka, Moscow, 1978), Pt. II.

[29] G. Iooss and D. D. Joseph, *Elementary Stability and Bifurcation Theory* (Springer-Verlag, New York, 1980).

[30] J. M. T. Thomson, *Instabilities and Catastrophes in Science and Engineering* (Wiley, New York, 1982).